The influence of carbon and oxygen on the magnetic characteristics of press-less sintered NdFeB magnets

Xia, Manlong; Abrahamsen, Asger Bech; Bahl, Christian; Veluri, B.; Søegaard, A. I.; Bøjsøe, P.; Millot, S.

Published in:
Journal of Magnetism and Magnetic Materials

Link to article, DOI:
10.1016/j.jmmm.2016.09.014

Publication date:
2017

Document Version
Peer reviewed version

The Influence of Carbon and Oxygen on the Magnetic Characteristics of Press-less Sintered NdFeB Magnets

M. Xia[1], A. B. Abrahamsen[2], C. R. H. Bahl[1], B. Veluri[3], A. I. Søegaard[3], P. Bøjsøe[4] and S. Millot[5]

[1]Department of Energy Conversion and Storage, DTU Risø Campus, Technical University of Denmark, Roskilde, Denmark
[2] Department of Wind Energy, DTU Risø campus, Technical University of Denmark, Roskilde, Denmark
[3]Grundfos A/S, DK-8850 Bjerringbro, Denmark
[4]Holm Magnetics APS, 2800 Kongens Lyngby, Denmark
[5]FJ Industries A/S, 5863 Ferritslev, Denmark
maxi@dtu.dk

Conference Paper #059

Corresponding author name : Manlong Xia

Corresponding author e-mail : maxi@dtu.dk / asab@dtu.dk

Preferred Journal (Journal of Magnetism and Magnetic Materials).

***Abstract*—The Pressless Process (PLP) was adopted to manufacture NdFeB sintered magnets, where the investigations on carbon and oxygen residues from heptane milling liquid media and graphite crucibles used for sintering were quantified to evaluate the influence on the magnetic characteristics. The carbon and oxygen content in the magnets produced from wet ball milling of strip cast flakes was found to be of the order 10^4 ppm and $4 \cdot 10^4$ ppm respectively, which resulted in soft magnetic behavior. However using jet milling the carbon and oxygen concentration were decreased by an order of magnitude resulting in coercivity of up to 829 kA/m. Thus the influence of the carbon from the graphite crucibles is small.**

***Index Terms*—NdFeB, Sintering, carbon, oxygen, α-Fe**

I. Introduction

The press-less process (PLP) was developed by Sagawa in 2008 with the aim to develop high coercivity magnets by preventing the increase of the oxygen content during the powder metallurgy process [1]. It was recommended by Sagawa to use graphite crucibles to hold loose jet milled NdFeB powder during alignment and and transport to the furnace for sintering [2]. As explained by Pan *et al.* [3], $Nd_2Fe_{14}B$ will react with carbon when mixing carbon powder with NdFeB powder and sintering at high temperature (700 °C – 1100 °C). The reaction can result in the α-Fe phase, neodymium carbides (Nd_2C_3, NdC_2), iron compounds (Fe_3C, Fe_3B) and additional phases. It illustrates that doping carbon in $Nd_2Fe_{14}B$ will influence the microstructure of the sintered NdFeB magnet. The magnetic properties of the phases mentioned above are shown in Table 1[4, 5]. It is known that both the α-Fe and Fe_3B phases have higher saturation magnetization than that of $Nd_2Fe_{14}B$, however, their anisotropy constants K_1 is much lower than the $Nd_2Fe_{14}B$ phase. Fe_3C has both lower saturation magnetization and anisotropy than $Nd_2Fe_{14}B$. Thus the magnetic properties of mixed compounds resulting from the reaction between $Nd_2Fe_{14}B$ and carbon are expected to be lower than NdFeB magnets. Besides, Nd-enriched carbides are formed and replace the Nd-rich (Nd_2O_3 or Nd metallic) phases in ordinary magnets, and will further reduce the coercivity of NdFeB magnets [6]. The graphite crucibles used in the press-less process are in contact with the NdFeB powder during sintering at high temperature (1000-1150 °C). For press-less sintering with graphite crucibles, it is a concern whether the carbon will enter the NdFeB sample and lead to complex reactions and compounds. Besides, when using the wet ball milling method with an organic liquid to produce the powder, the carbon from organic compounds like heptane may react with the NdFeB powder at higher temperature without suitable treatment. The oxygen in the organic compounds may also react and cause more complex phases. It is known that the carbon and oxygen from paraffin wax and polyethylene will destroy the microstructure and properties of NdFeB magnets in Metal Injection Molding process [7]. It is necessary for a discussion on how carbon and oxygen influence the NdFeB magnet in the press-less process due to milling medium and graphite crucible.

	$Nd_2Fe_{14}B$	$Dy_2Fe_{14}B$	α-Fe	Fe_3B	Fe_3C

M_s(T)	1.61	0.71	2.15	1.62	1.36
K_1(MJ m^{-3})	4.9	4.5	0.046	-0.32	0.45

Table 1. The properties of the main and possible secondary magnetic phases of the sintered NdFeB magnets [4, 5]

In this paper, we investigate the carbon and oxygen content of NdFeB magnets made by both a) wet ball milling of NdFeB hydrides in heptane and b) jet milling followed by subsequent sintering of the powder in graphite crucibles. The microstructure and magnetic properties of magnets produced by both methods are presented in this paper. A discussion on the carbon and oxygen influence on NdFeB magnets will be given.

II. EXPERIMENTS

A commercial N35UH magnet, strip cast flakes (composition: $Nd_{12.86}Dy_{1.64}Fe_{76.65}B_{5.79}$ (at%)) and six isotropic PLP samples based on the strip cast flakes were used to measure the carbon and oxygen content. The first three PLP samples were prepared by wet ball milling of hydrides of the strip cast flakes in heptane for 12 h using Pulverisette 7hign energy ball mill. The typical mass of the powder for milling was 10 g and 100 g of steel balls of Ø3 mm diameter were added into the 80 ml jar before the milling., The ball milled powder had a typical diameter of ~ 6 μm and was dried by connecting a vacuum pump to the gas valve of the ball milling jar. . The mechanical pump provided a vacuum in the order of 10^{-1} mbar, but the outlet of the vacuum pump was connected to a liquid trap preventing back streaming of oxygen from the ambient atmosphere. Secondly the pumping system was flushed with 99.9 % argon several times to reduce the presence of oxygen. The ball mill jar was transferred to an argon filled glove box after the drying and 1.5 g of the powder was tapped into graphite crucible of inner diameter Ø7 mm and length 14 mm. The sintering procedure started with evacuating the furnace to 10^{-4} mbar and ramping to the final sintering temperature. The wet milled sample were sintered at at 1090 °C , 1110 °C and 1130 °C for 2 h in vacuum (W1090, W1110 and W1130) and the cooling rate was 25 °C/min. The three Jet milled samples were prepared using ~ 5 μm size powder. A Micromazinacione spiral jet mill equipped with Impakt™ powder feeder by Powder and Surface GmbH was used for the milling in nitrogen. Subsequently the powders were transfered to graphite crucibles and sintered at 1090 °C , 1110 °C and 1130 °C for 2 h in vacuum (J1090, J1110 and J1130). The carbon content of the samples was measured by a carbon analyzer CS-800 from ELTRA GmbH which requires approximately 1 g of material. The magnetic properties of the samples were characterized in a cryogenic vibrating sample magnetometer (VSM) from Cryogenic Ltd. By measuring the shape of the samples, demagnetize factor N were calculated and used to determine the internal field H_i. The mass of samples m was used to normalize the magnetization curves [8]:

$$H_i = H_a - NM \qquad (1)$$

$$M = \frac{m}{\rho_{NdFeB}} \qquad (2)$$

where H_a is the applied field and ρ_{NdFeB} = 7.4 g/cm^3 is the assumed mass density of fully dense magnets.

The microstructure was investigated by scanning electron microscopy (SEM/EDS) using a TM3000 from Hitachi. The area percentage of the phases in the microstructure is calculated using ImageJ by the color of the phases.

III Results and discussion

Before sintering the powders were compacted into cylinders with diameters of 7.74 mm and filled to a length of approximately 13 mm, which resulted in a packing density if about 3 g/cm^3. After sintering, the press-less samples shrinks to diameters of 6-7 mm and lengths of 7-9 mm, depending on the different sintering temperatures. Higher sintering temperature results in more shrinkage. For a full dense sample, the shrinkage ratio (final volume / initial volume) is 0.41. The carbon and oxygen contents of all samples are given in Table 2. The samples prepared by jet milled powder (J) have almost the same carbon content as the commercial magnet N35UH at the lowest sintering temperature of 1090 °C and about twice as much at the highest temperature of 1130 °C. The oxygen content is varying between 3000-6100 ppm. The carbon from the graphite crucibles therefore seems not to have much reaction with the $Nd_2Fe_{14}B$ phase at high temperature. The carbon and oxygen content of the starting strip cast flakes is about a factor of 10 lower than the level of the commercial magnet. It illustrates that the carbon from the graphite crucible reacts with $Nd_2Fe_{14}B$ at high temperature, although only weakly, because carbon in the form of graphite seems chemically inert. Regarding the oxygen content, graphite is known to out-gas absorbed oxygen, which could contaminate the NdFeB samples during sintering. Since all six press-less samples use the same graphite crucibles, the influence of the oxygen out-gassing is the same for all the samples and the difference in the oxygen content of the samples is mainly due to other reasons, e.g. the heptane.

The wet ball milling samples all have significantly higher carbon and oxygen content in the range of 9500-11000 ppm and 4.3-4.8 % respectively. Since the carbon from the graphite crucibles has been shown to only enter NdFeB to a limited degree during sintering, the carbon in the W1090, W1110 and W1130 samples must come from the heptane used during the ball milling procedure, similar to the addition of pure carbon powder to the NdFeB powder in [3]. The oxygen content is also very high, which is might be dissolved in the heptane or be caused by the relative high pressure during the drying procedure. It is believe that the finely dispersed carbon and oxygen in the wet milling media is causing a large internal reaction surface to the NdFeB powder compared to the graphite crucible only exposing the outer surface of the NdFeB sample.

	Strip cast	Wet ball milled (W)			Jet milled (J)			N35 UH
		1090ºC	1110	1130	1090	1110	1130	
C (ppm)	110	9578	11066	10320	1249	1655	2182	1272
O (ppm)	220	48121	44979	43913	2590	6101	3066	1223

Table 2. The measured carbon and oxygen content of samples based on wet ball milled (W) and jet milled powder (J) sintered at different temperatures.

Fig. 1 shows the backscattered electron SEM images of the wet and jet milled samples sintered at 1130 °C (W1130 and J1130). Three phases are observed in the microstructure of W1130: a dark phase, a grey phase and white phase. The dark phase occupies 26 % of the image area whereas the gray is the majority phase. Fig. 2 shows the EDS mapping of Nd and Fe for a selected part of the wet ball milled sample. It is seen that Nd is concentrated in the white phase, but it is also seen in the grey phase. The dark phase seems not to include much Nd. A similar Fe mapping is shown in Fig. 2 and indicates that Fe is richest in the dark phase, but also present in the grey phase. The white phase contains very little Fe. The quantitative composition of each phase of Fig. 2 are listed in Table 3 and confirm the mapping results. It is interesting that the Dy atom percentage in the grey phase and dark phase are 5.4 and 5. The Dysprosium distribute averagely in both phases, which is different from Neodymium. It may be due to the Lα peak of Dy is overlapping with Fe Kα peak and some Fe's content is calculated as Dy's content, which gives a wrong quantitative results of Dy's content for high Fe content in both phases. The dark phase shows a high Fe concentrated and a high Fe/Nd ratio of 191.89 indicating that it is probably α-Fe, Fe_3B or Fe_3C. These phases occupy approximately 26 % of the surface area of W1130 and are expected to act as soft magnetic materials as outlined in table 1. The grey color phase is most likely the $Nd_2Fe_{14}B$ hard magnetic phase since the Fe/Nd ratio is 8.11 being close to the stoic metric ratio of 7/1. The grain size of the $Nd_2Fe_{14}B$ phase in the wet ball milled sample of fig 1 and 2 is in the order of 10-40 μm and thereby relatively too large. Secondly no thin grain boundaries are observed between the grains. Thin grain boundaries are expected to be the main feature preventing magnetic domain wall movement and the coercivity is therefore expected to be low. The magnetization curves of the wet ball milling samples in Fig. 3 confirm a soft magnetic behavior.

In Fig.3, with increasing sintering temperature, the sample's saturation magnetization is increased. If we assume the dark phase of fig. 1 is just α-Fe and the remaining phases are $(Nd, Dy)_2Fe_{14}B$ and the Nd-rich phase, then a fit could be done to the curves in Fig.3. The α-Fe have a saturation magnetization J_s (α-Fe) = 2.15 T and a very small anisotropy constant K_1 = 0.046 MJ m^{-3}. Since there is no coercivity in the magnetization curves, it could assume that the magnetization is just a sum of the magnetization of the pure phases including α-Fe phase. The magnetization of a phase with index i showing a soft magnetic behavior can be described by the Weiss model [9]:

$$\mu_0 M_i = V_i J_{S,i} \tanh\big(a_i(H + b_i)\big) \qquad (3)$$

where $J_{S,i}$, a_i and b_i are the saturation magnetization and the parameters describing the properties of phase i. The volume fraction of phase i is denoted V_i. By also including a susceptibility term to the magnetization, then the final fitting equation can be written as:

$$\mu_0 M = (1 - V_{\alpha-Fe})J_1 \tanh\big(a_1(\mu_0 H + b)\big) + V_{\alpha-Fe} J_{\alpha-Fe} \tanh\big(a_2(\mu_0 H + b)\big) + \chi * \mu_0 H \qquad (4)$$

where χ is the susceptibility of the magnetization curves and $V_{\alpha\text{-Fe}}$ is the volume fraction of the α-Fe phase. The fitting results are

shown in Fig. 3b and Table 4. It was found that $V_{\alpha\text{-}Fe}$ of α-Fe are almost the same for the different sintering temperature found from the microstructure images of the samples. The saturation magnetization J_1 of other phases (Nd, Dy)$_2$Fe$_{14}$B and the Nd-rich phase increase from 0.55 T to 0.89 T, which illustrates that the percentage of (Nd, Dy)$_2$Fe$_{14}$B phase increases with the temperature, because the Nd-rich phase is non-magnetic and the (Nd, Dy)$_2$Fe$_{14}$B phase has a saturation magnetization of 1.51 T. However, the reaction between carbon and Nd$_2$Fe$_{14}$B will produce a complex mixture of compounds at higher temperature since the white color phase (Nd-rich phase) play an important role in these samples.

We selected five white phase grains to characterize the quantitative atomic percentage of elements in Fig 2. It seems that Fe/Nd varies from 0.08 to 0.51 for different part of the white phases in Table 3, which is indicating an inhomogeneous composition. It seems that the reaction between carbon and NdFeB leads to complex defects in the magnets, which may be a reason why the final sample shows no coercivity.

The J1130 sample prepared by jet milling shows only a small fraction of dark phase in the microstructure in Fig.1. These dark phases seem to be defects and not a phase. The grey and white phases are also observed in the microstructure of the J1130 sample. Element mapping in Fig. 4 shows that the Nd is rich in the white phase. The quantitative EDS results in Table 5 show that the grey phase is probably Nd$_2$Fe$_{14}$B phase and the white phase is Nd-rich phase identified by the Fe/Nd ratio. The white phase 1 and 2 have similar Fe/Nd ratio (3.23 and 2.53) and are much higher than that of the white phase in W1130 sample. Besides, the Nd-rich phase in the jet milling sample is not as pronounced as in the wet ball milling sample. It indicates that the jet milling samples will have different magnetic properties. The samples J1090, J1110, J1130 show high coercivity (687, 368, 829 kA/m) and hard magnetic properties in the magnetization curve of Fig. 5. The carbon did not react much with the Nd$_2$Fe$_{14}$B phase during the PLP sintering of the jet milling powder, which resulted in successful samples. Additionally, the oxygen content of the J1110 sample is 6101 ppm, which is the highest of all three jet milled sample. The J1110 sample has lowest coercivity (368 kA/m) of all three samples. The higher oxygen content, the lower coercivity is observed in Fig. 5. For the jet milled samples the oxygen has a larger influence on the magnetic properties than carbon when using the press-less process.

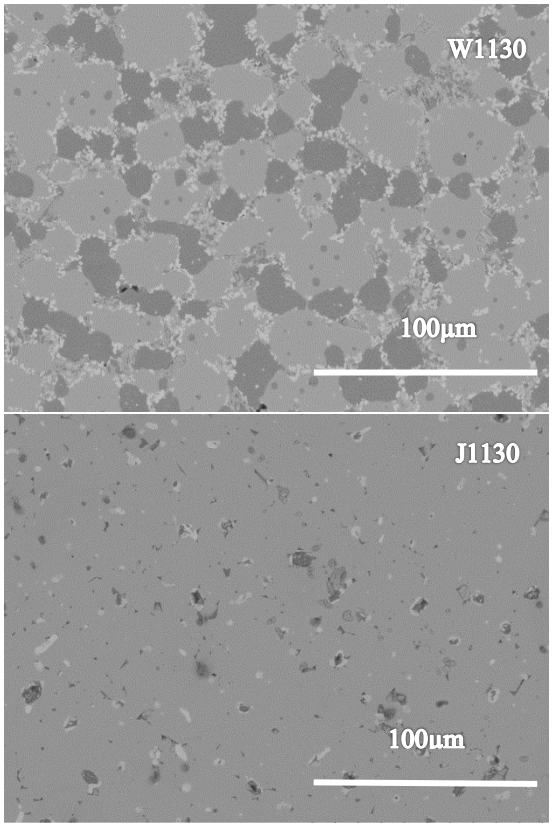

Fig.1. The microstructure of W1130 (4 wt% Dy wet ball milling sample sintered at 1130 °C) and J1130 (4 wt% Dy jet milling sample sintered at 1130 °C).

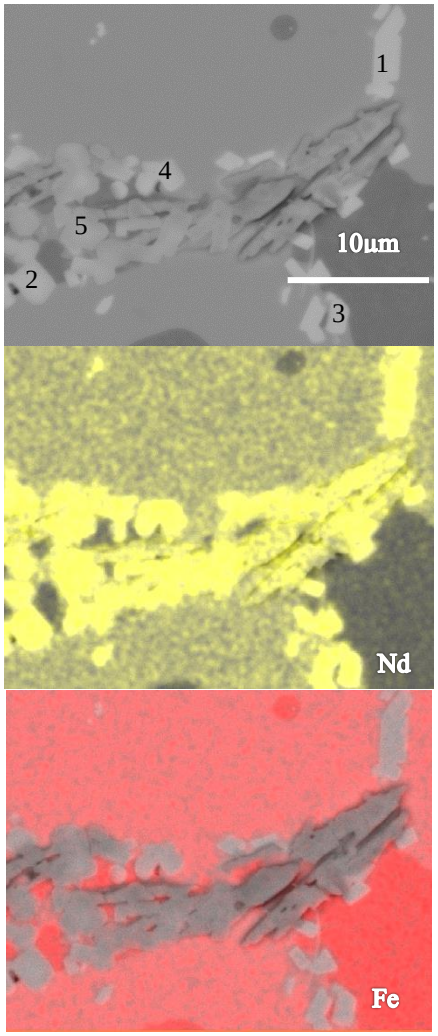

Fig.2. The SEM image and EDS mapping of Nd and Fe in the W1130 sample.

Atom percentage (%)	Nd	Fe	Dy	Fe/Nd
White phase 1	30±2	6.4±0.2	3.6±0.3	0.21
White phase 2	27±2	13.7±0.4	2.1±0.2	0.51
White phase 3	32±2	5.4±0.2	3.5±0.3	0.17
White phase 4	35±2	2.80±0.08	2.4±0.2	0.08
White phase 5	25±2	2.43±0.09	2.6±0.2	0.10
White phase Average	30±4	6±4	2.8±0.6	0.2
Grey phase	7.4±0.7	60±2	5.4±0.6	8.11
Dark phase	0.37±0.06	71±3	5±1	191.89

Table 3. The quantitative EDS results of W1130 sample in Fig.2 (The white phase analysis was done in 5 selected points of fig 2.).

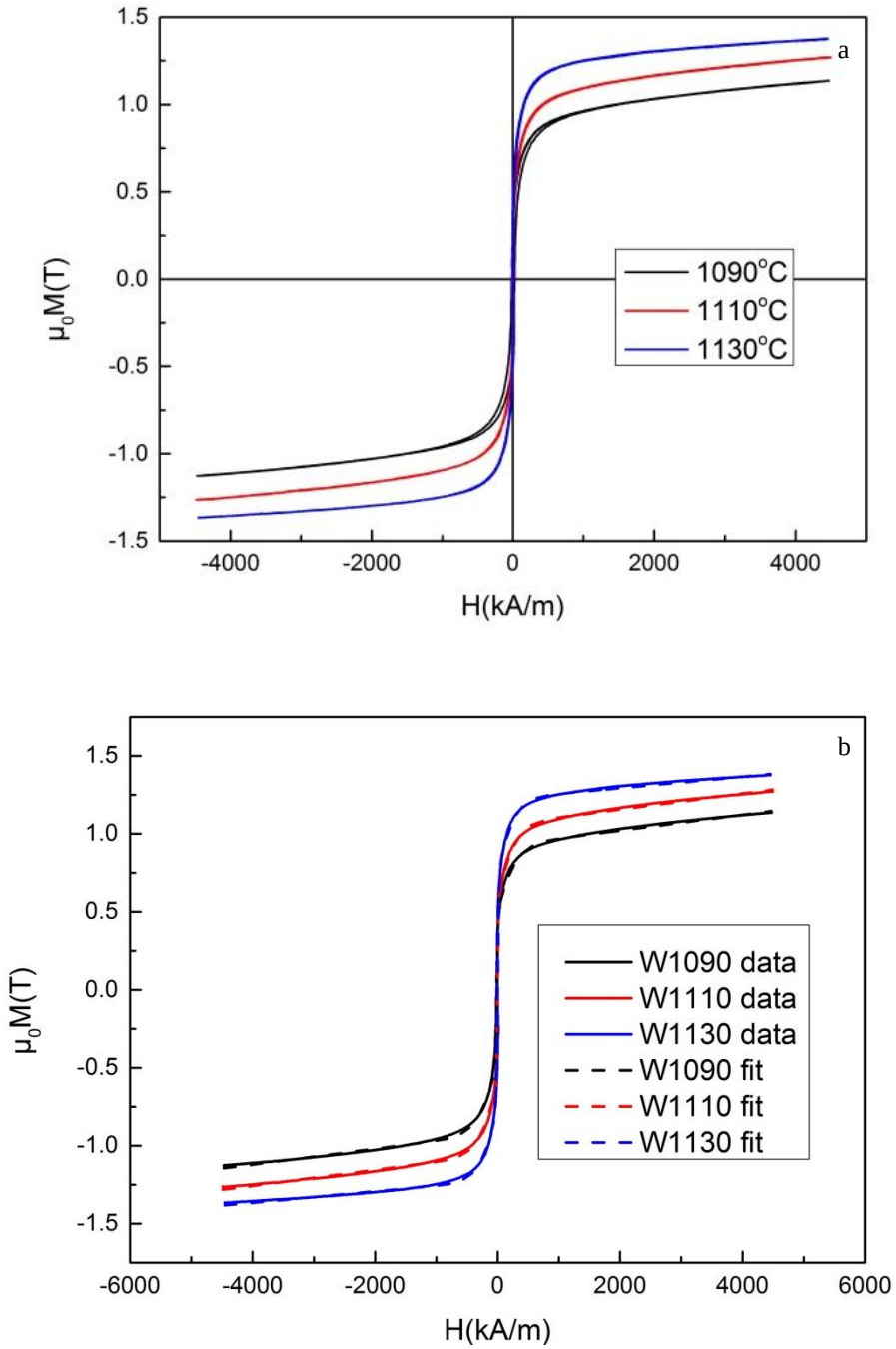

Fig.3. a) The magnetic properties of 4 wt% Dy sample (W1090, W1110, W1130) prepared by wet ball milling and sintered at different temperatures. The applied field has been corrected for the demagnetization factor in equation (1). b) The fit of the magnetization curves of the wet ball milling samples.

	$\mu_0 M = (1 - V_{\alpha-Fe})J_1 \tanh(a_1(\mu_0 H + b)) + V_{\alpha-Fe} J_{\alpha-Fe} \tanh(a_2(\mu_0 H + b)) + \chi * \mu_0 H$				
Fit parameter	$V_{\alpha\text{-Fe}}$ (%)	J_1(T)	χ	a_1(T^{-1})	a_2 (T^{-1})
W1090	23	0.548(2)	0.041(4)	45.6 (8)	2.85(3)
W1110	27	0.6466(7)	0.041(1)	77(2)	3.184(8)
W1130	26	0.889(7)	0.030(2)	42(2)	3.28(2)

Table 4. The fit results of magnetization curves of the wet ball milling samples: W1090, W1110 andW1130.

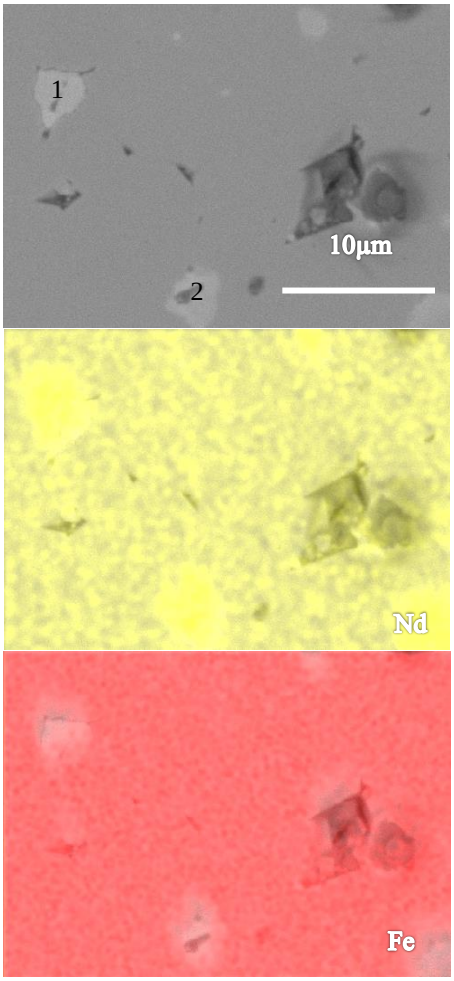

Fig.4. SEM image and EDS mapping of Nd and Fe in the J1130 sample.

Atom percentage (%)	Nd	Fe	Dy	Fe/Nd
White phase 1	13±1	42±1	2.8±0.3	3.23
White phase 2	17±1	43±1	1.2±0.1	2.53
Grey phase	7.7±0.7	61±2	2.8±0.3	7.92

Table 5. The quantitative EDS results of J1130 sample prepared by jet milling of the strip cast flakes and shown in Fig.4 (white phases are discrete in Fig.4 and two white phases were chosen to do quantitative EDS).

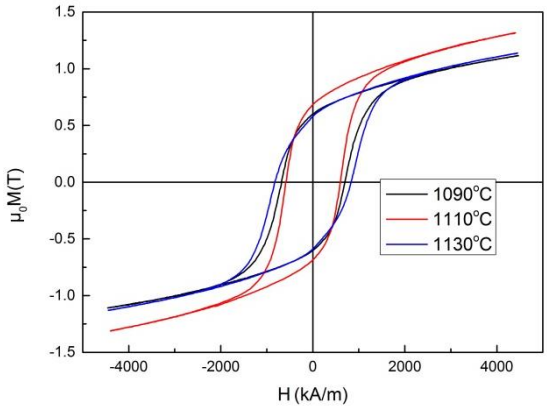

Fig.5. The magnetic properties of 4 wt% Dy sample (J1090, J1110, J1130) prepared by jet milling and sintered at different temperatures. The applied field has been corrected for the demagnetization factor in equation (1).

Comparing the microstructure of W1130 and J1130, it is seen that carbon has probably reacted with $Nd_2Fe_{14}B$ phase at high sintering temperature as in literature. However, the reaction is much more pronounced for the carbon added by the liquid heptane used in the wet ball milling as from the carbon from the graphite crucibles. Using graphite crucibles in the press-less process does not seem to influence the NdFeB magnets. The oxygen will influence the magnetic properties of the ample more. If we use wet ball milling to prepare press-less NdFeB magnet, the separation of organic compounds with NdFeB powder is necessary. Otherwise, when carbon reacts with the NdFeB powder it results in soft magnetic phases α-Fe or Fe_3B, even though $Nd_2Fe_{14}B$ exists, it will show no coercivity at all.

III. CONCLUSION

It is found that magnets produced by wet ball milling of strip cast NdFeB flakes in heptane and subsequently sintering in graphite crucibles have a carbon and oxygen concentration of the order of 1 and 4 %, which is resulting in soft magnetic behavior. However using jet milling the concentration of carbon and oxygen was decreased by an order of magnitude and hard magnetic behavior was obtained showing a coercivity up to 829 kA/m. This is indicating that the carbon from the graphite crucible has a small influence on the magnetic properties.

Acknowledgement

This work is part of the REEgain Innovation Consortium funded by the Innovation Fund Denmark (www.REEgain.dk)

REFERENCES

[1] M. Sagawa and Y. Une, "A new process for producing Nd–Fe–B sintered magnets with small grain size," Proc. 20th Int. Workshop on Rare Earth Permanent Magnets and Their Applications, Crete, 2008, pp. 103–105.

[2] M. Sagawa, "Process for producing sintered NdFeB magnet and mold for producing sintered NdFeB magnet", EP 2,187,410 (A1), May 19,2010 Bulletin 2010/20

[3] F. Pan, M. Zhang, R. F. Zhao, B. X. Liu and M. Tokunaga, "Some new Nd-rich carbides formed by solid state reaction of $Nd_2Fe_{14}B$ and carbon" J. Phys. D: 31 (1998) 488-493.

[4] J. M. D. Coey, "Hard Magnetic Materials: A Perspective" IEEE Transactions on magnetics, vol. 47, NO. 12, December 2011.

[5] T. Schrefl, D. Süss, W. Scholz, J. Fidler, ''Finite element simulation of hard magnetic properties'' Proc. PAMM Conference, Chicago, 2000.

[6] T. T. Sasaki, T. Ohkubo, Y. Une, H. Kubo, M. Sagawa and K. Hono, "Effect of carbon on the coercivity and microstructure in fine-grained Nd-Fe-B sintered magnet" Acta Materialia 84 (2015) 506-514.

[7] L. U. Lopes, M. A. Carvalho, R. S. Chaves, M. P. Trevisan, P. A. P. Wendhausen, H. Takiishi, "Study of carbon influence on magnetic properties of metal injection molding Nd-Fe-B based magnets", Eighth International Latin American Conference on Powder Technology, November 06 to 09, 2011, Brazil.

[8] A. Aharoni, "Demagnetizing factors for rectangular ferromagnetic prisms" Journal of Applied Physics 83, 3432 (1998).

[9] S. Blundell, "Magnetism in condensed matter" Oxford University Press, 2001 and ISBN 978 0 19 850592 1

[10] H. Hauser, R. G. Grössinger, "Hysteresis model for isotropic magnetization process-application and physical interpretation" Journal of Magnetism and Magnetic Materials 226-230 (2001) 1254-1256